



Estimation of microwave resonant measurements uncertainty from uncalibrated data

K. Torokhtii¹, A. Alimenti¹, N. Pompeo¹ and E. Silva¹

¹Department of Engineering, Roma Tre University, Via Vito Volterra, 62, 00146 Roma, Italy

ABSTRACT

We present an extended study on the uncertainty in resonant measurements. The uncertainty of the resonant frequency and quality factor was estimated. Two different measurement systems and different fitting approaches were used. The effect of the use of uncalibrated resonant curves on uncertainty was extensively studied. For the uncalibrated data the systematic contribution to the uncertainty was determined.

Section: RESEARCH PAPER

Keywords: Dielectric resonator, Microwaves, Uncertainty

Citation: K. Torokhtii, A. Alimenti, N. Pompeo and E. Silva, Estimation of microwave resonant measurements uncertainty from uncalibrated data,, Acta IMEKO, vol. A, no. B, article C, Month Year, identifier: IMEKO-ACTA-A (Year)-B-C

Section Editor: name, affiliation

Received month day, year; **In final form** month day, year; **Published** Month Year

Copyright: This is an open-access article distributed under the terms of the Creative Commons Attribution 3.0 License, which permits unrestricted use, distribution, and reproduction in any medium, provided the original author and source are credited.

Corresponding author K. Torokhtii, e-mail: kostiantyn.torokhtii@uniroma3.it

1. INTRODUCTION

Continuous interest in the microwave measurements leads to the realization of the industrial grade methods for the material characterization. A wide range of material properties could be characterized at microwaves. One of the advantages of microwave techniques is their high sensitivity. They are widely used for the measurements of the complex permittivity of liquids [1] and solid dielectrics [2]. Since long time microwave techniques have been used for the surface impedance (of Z_S) measurements of conductors. In particular, the microwave dielectric resonator (DR) method is a standard for the measurements of Z_S of superconductors [3]. In connection with other techniques as d.c. measurements, it is able to show a detailed picture of the microscopic properties of superconductors [4]. In this article, we focus on the DR based measurement technique.

In the last years, Vector Network Analysers (VNA) became more accessible due to low-cost solutions [5][6]. However, the quality of the measurements relies heavily on the calibration procedure. In the case of less-performant VNAs, the importance of calibration becomes even more relevant.

In some cases, calibration becomes an impossible operation. The notable case is when the device under test (DUT) is placed in a harsh or particularly difficult environment. An example is represented by measurements of materials or devices at low,

cryogenic temperatures [7][8]. Apart from the complexity of the cryogenic measurement system, one of the main problems originates from the part of the microwave line inside the cryostat which could not be calibrated using the standard procedure. Here, the main role is played by the absence of microwave standards capable to keep their characteristics in the hostile environment. One of the solutions is to develop custom standards [9], but it often requires very advanced techniques and particular knowledge. Moreover, it becomes rather difficult to associate the appropriate uncertainty with the measured quantity.

In this paper, we extend the analysis of the effect of the uncalibrated measurements [10][11] to have a more complete generalized picture of the resonant parameters. We focus our attention on the resonant frequency (f_0) and quality factor (Q). Here we explore the impact of different VNAs and fitting methods on the estimation of uncertainties on Q and f_0 . A key objective of the study is the determination of the uncertainty to be associated to Q and f_0 for measurements where no calibration could be performed. For the measurements we use the Hakki-Coleman (H-C) dielectric resonant system described in [10][11].

2. VARIABLE-Q RESONATOR CELL

In this study, we aim to evaluate the measurement uncertainty on Q and f_0 when a microwave line, or a part of it, cannot be calibrated, as in the cryogenic scenario above depicted. We designed an “open” type H-C resonator operating at room

temperature. We used phase stable microwave cables with female-female connectors. We designed the DR cell to have the reference plane of the microwave cable connector near the edge of the cell. Coupling was made by removable antennas inserted directly in the cable connector. With this design, we were able to perform the calibration up to the reference plane of the cable connectors. The DUT consists therefore in the resonator cell only, as desirable in an ideal setup. In this way we are able to directly compare uncalibrated measurements with calibrated ones without any not-accounted contribution and without the need for a de-embedding procedure [12].

In Figure 1 the sketch of the measurement cell is shown. The dielectric resonator is cylindrical and loaded with a sapphire puck, chosen because of its low dielectric losses and high permittivity. The latter allows to concentrate the electromagnetic field within and near the dielectric puck. A mono-crystal sapphire puck with diameter 8.0 ± 0.1 mm and height 4.5 ± 0.1 mm was used. An Anritsu 37269D VNA and a R&S ZVA-40 VNAs with phase stable Anritsu cables were used for measurements and connections.

We are interested in the evaluation of the uncertainty in the measurements of the resonator parameters with different quality factors Q . We then designed a system for measurements in a wide range of Q factors in the same conditions, which include, in particular, the frequency range of operation of the DR.

In order to change the Q values of the resonator in a controlled way, we could substitute the bases using metals with different resistivities and change the position of the upper base, and thus the height of the corresponding gap of the DR. By fine tuning the latter, we were able to keep the resonant frequency within a chosen fixed range, 13.0 ± 0.5 GHz.

3. Q-FACTOR AND RESONANT FREQUENCY EXTRACTION

Q and f_0 are important properties of a resonator. A good example is the resonant technique to measure the surface impedance of a material $Z_S = R_S + iX_S$ here R_S and X_S are the surface resistance and surface reactance, respectively. In this measurement technique the quality of measurements of the surface impedance by the resonant method depends directly on f_0 and Q . Usually, the variation of the surface impedance with some external parameter is obtained experimentally, while the determination of the absolute value of Z_S is a more complex issue due to the absence of the reference material with known X_S . The

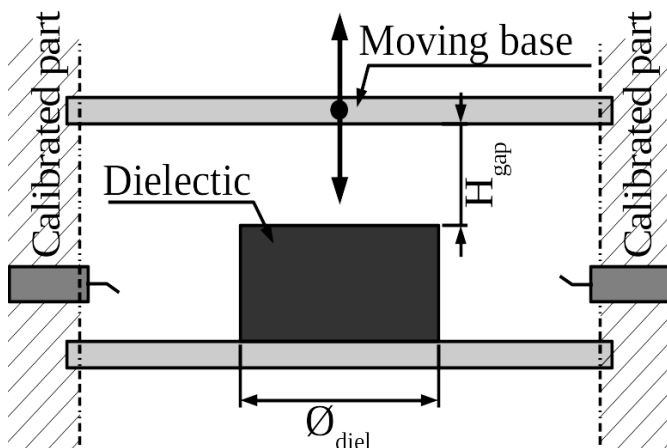


Figure 1. Variable- Q resonant cell.

relation between Z_S and resonant parameters is the following [13]:

$$\Delta Z_S = \Delta R_S + i\Delta X_S = G\Delta \frac{1}{Q} - 2iG \frac{\Delta f_0}{f_0} + bg, \quad (1)$$

where G is a constant called geometrical factor, and the background “ bg ” is the contribution of the resonator without the sample. From equation (1) it is clear how the uncertainty of Z_S originates mainly from $u(Q)$, Q , $u(f_0)$ and f_0 ($u(G)$, as obtained by simulation, is usually $<1\%$), whence the interest in the estimate of $u(Q)$ and $u(f_0)$.

In a resonator working in transmission f_0 and Q can be obtained based on the measurements of the complex-valued transmission coefficient, S_{tr} . While preliminary estimates for Q and f_0 can be obtained by the so-called -3dB method, a more precise approach is to use an appropriate fit of the resonance curve. In [14] it was shown that a Lorentzian curve can be used to fit the function $|S_{tr}(f)|$ only for “ideal” cases. The real resonator includes corrections connected to cross-coupling and phase contributions. The resonance curve can be described through the following equation (“Fano resonance model” [15]) with a phase correction:

$$S_{tr}(f) = \left[\frac{S_{tr}(f_0)}{1 - 2iQ \frac{f - f_0}{f_0}} + S_c \right] e^{i\varphi}, \quad (2)$$

where $S_{tr}(f_0) > 0$ is the transmission S -parameter at the resonant frequency, S_c represents the contribution originated from the cross-coupling between the resonator ports and $e^{i\varphi}$, with $\varphi = \alpha + \beta f$, takes into account the propagation phase delay along the line.

There is a large number of methods for the extraction of f_0 and Q from the experimental data [16]. A widely used method is the so-called circular fit approach [17], but it is also possible to use a complex-valued modification of the Levenberg-Marquardt algorithm to fit the complex S_{tr} [18]. However, complex-valued fitting requires more calculation power and custom algorithms. Additional complexities arise when the uncertainty of the fitting parameters must be estimated. From this point of view, the fit of the modulus of S_{tr} remains more accessible due to already implemented algorithms in popular programming languages such as Python and MATLAB [19]. Using the fit of $|S_{tr}(f)|$ one can implement a fitting procedure with cheap computers like the Raspberry Pi. $|S_{tr}(f)|$ is obtained from equation (2) as:

$$|S_{tr}(f)|^2 = \frac{S_{tr}(f_0)}{1 + 4Q^2 \left(\frac{f - f_0}{f_0} \right)^2} \left[S_{tr}(f_0) + 2\text{Re}(S_c) + 4Q \frac{f - f_0}{f_0} \text{Im}(S_c) + \text{Re}^2(S_c) + \text{Im}^2(S_c) \right] \quad (3)$$

This fit requires only 5 independent parameters.

Since a VNA allows the measurement of the S -parameters as complex quantities, a fit of the complex quantity $S_{tr}(f)$ could also be devised, yielding also the additional information concerning the phase correction $e^{i\varphi}$. Hence, differently from [11], here we additionally perform a complex fit of equation (2) and we make a comparison of the results that can be obtained

through both approaches. Resorting to standard algorithms which usually accept only real quantities in input, here we use a particular approach to fit complex data and include also experimental data uncertainty. To do so, we define the objective function to be minimized by separating the real and imaginary parts of S_{tr} , each with its experimental uncertainty. Hence, each measured S_{tr} curve, composed of n data points, becomes an array of $2n$ data points with the first half given by the real parts and the second by the imaginary parts. Correspondingly, the fit function is given by the real and imaginary parts of equation (2) for the first and second half of the measurement data set, respectively. As a consequence, differently from the fit to equation (3), the fit is done with 7 independent parameters.

4. MEASUREMENT PROCEDURE

In this section, we present an extended elaboration of the measurement procedure presented in [10]. The aim is to complete the estimate of the uncertainty of the measurements of the characteristic parameters of a resonator for uncalibrated measurements, including also the resonant frequency.

We performed experimental measurements in a wide range of Q factors, namely 1500 - 9500, with very small variations of other controlled parameters of the resonant system. The interest is the comparison between the Q and f_0 measurements obtained with and without the VNA calibration. Measurements were done using two different VNAs, the Anritsu 37269D and the R&S ZVA-40, to assess the robustness of the results among different instruments. Indeed, this point is not trivial, since the uncalibrated curves contains un-removed contributions originating also from the internal VNA circuitry, which in calibrated measurements is transparently removed by the calibration.

First, we fixed the calibration in the narrow frequency band 12.5-13.5 GHz, chosen to accommodate all the resonant curves (with different Q) to be measured with sufficient density of frequency points. Measurements were performed with 1601 calibrated points with the Anritsu 37269D VNA (the maximum number of data-points) and 32000 calibrated points with the R&S ZVA-40. The calibration was performed by the standard 12-term SOLT (Short-Open-Load-Thru) procedure by the algorithms incorporated in both VNAs. For the experimental measurements, we followed Anritsu 37269D and R&S ZVA-40 standard calibration guides. Resonance curves were then recorded with Q -factor varied in the range $1500 < Q < 9500$. To obtain such a wide range of Q with the same setup we change the air gap and we use different metals for the bases, as explained before. The gap, controlled by only one movable part of the resonator cell—the upper base (See Figure 1), allowed to tune the operating resonance frequency to be always within the frequency range of the calibration.

For each fixed position of the upper base, two measurements were performed: with and without the calibration. In Figure 2 an example of the measured calibrated and uncalibrated resonant curve is shown for Anritsu 37269D (left panels of Figure 2) and R&S ZVA-40 (right panels of Figure 2). The difference is immediately appreciated, confirming the need to assess the quality of an uncalibrated measurement even for a resonant device (naïvely, one could expect that resonant systems are sufficiently narrowband to be nearly insensitive to the calibration).

5. RESULTS

A series of resonant curves (~ 40) was recorded and fits by equation (1) (complex fit) and equation (2) (fit of the modulus) were applied to uncalibrated and calibrated data. Care was taken to have similar fit conditions. It should be noted that in our situation, in each curve the measured points were evenly spaced in frequency for all measurements. Since Q changes significantly, without proper “normalizations” the fits of the curves with low and high Q would not be in the same conditions for what concerns the density of information per interval.

Therefore, we proceeded as follows. First, we limited the span of each curve to $N\Delta f_{FWHM}$, where Δf_{FWHM} is the full-width half maximum frequency range, and $N > 1$ is a proper multiplicative factor. In our case, N was constrained by the available frequency range of the calibration and requirements to be the same for all experimental curves. As a result, we choose $N = 4$. The resulting curves, having different frequency spans with frequency points evenly spaced, had at this step different numbers of points. Each set was then trimmed uniformly, in order to have as much as possible the same amount of evenly spaced data-points. As a result, in the range of $Q = 1500 - 9500$ we obtained the final set of the resonant curves, trimmed and with same information density, with span $4\Delta f_{FWHM}$ and the number of data-points near 300. We now discuss the elaboration of this set of curves.

Concerning the uncertainties, it should be noted that the uncertainty $u(S_{tr})$ could be estimated only for the calibrated curve [11]. In particular, for the Anritsu 37269D these estimations could be given by the “Exact Uncertainty Calculator” - proprietary software tool by Anritsu [20] (although alternative tools like in [21] could be used). This tool estimates automatically the uncertainties for all S -parameters taking into account the characteristics of the VNA, cables, connectors and calibration kit. For R&S ZVA-40, on the other hand, the uncertainty was obtained from the general specifications of the VNA provided in the datasheets. Hence, the uncertainty for R&S ZVA-40 is not accurately tailored to the measurements and should be

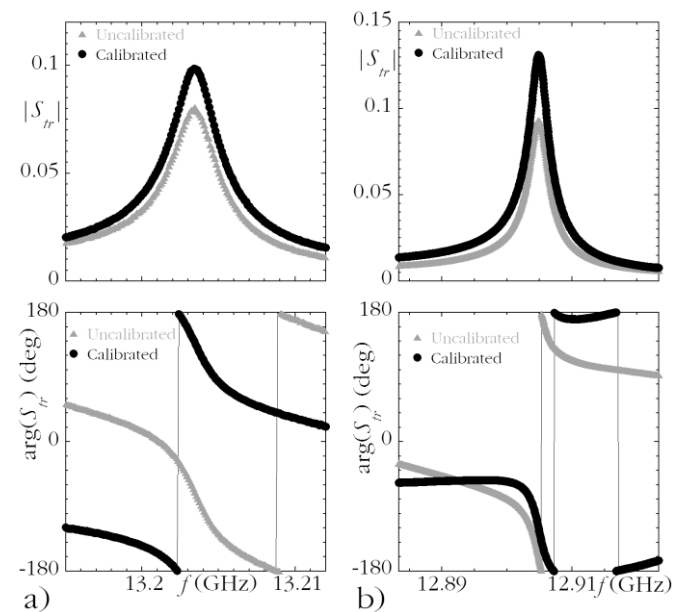


Figure 2. Measured resonant curves with and without calibration applied in modulus (upper panels) and phase (lower panels). Panels a: Anritsu VNA; panels b: R&S VNA.

considered as an over-estimated, worst case figure. For both VNAs the estimation of $u(S_{tr})$ is provided in form of dependencies of the uncertainties of $u(|S_{tr}|)$ and $u(\arg(S_{tr}))$ on $|S_{tr}|$. Thus, separate uncertainties should be assigned for each measured point yielding additional complications in the fit procedure. Moreover, since the uncertainties are provided on the modulus and phase, the uncertainties on real and imaginary parts of S_{tr} needed for the complex fit were derived by the uncertainty propagation. In the calibrated conditions, the worst case of measurement uncertainty on S_{tr} , was $<1.7\%$ for modulus and $<0.5\%$ for phase for Anritsu 37269D and $<2.4\%$ in modulus, $<1.6\%$ in phase for R&S ZVA-40. For uncalibrated curves, zero uncertainty on S_{tr} had to be used in absence of further information.

A widely used Levenberg-Marquardt [18] fit algorithm implementation in Python provides a variance vector of the fit parameters through the numerically calculated Jacobian (more details can be found in refs. [19][22]). Q and f_0 uncertainties were estimated as the square root of the corresponding fitting parameter variances.

Moreover, as a consequence of the non-application of the calibration, additional significant sources of uncertainty are expected. Thus, we define as a measure of this uncertainty the discrepancy between the resonant parameters as derived by the fitting of calibrated and uncalibrated curves. The discrepancy of Q could be defined as the relative variation between Q obtained from calibrated (Q_{cal}) and uncalibrated (Q_{uncal}) data, $D_Q = (Q_{uncal} - Q_{cal})/Q_{cal}$. For f_0 the discrepancy is defined in the same manner as $D_{f_0} = (f_{0,uncal} - f_{0,cal})/f_{0,cal}$ where $f_{0,uncal}$ and $f_{0,cal}$ are resonant frequencies obtained by the fit of uncalibrated and calibrated curves, respectively.

In Figures 3a and 4a the relative uncertainties (u_r) of Q -factors and resonant frequencies f_0 are shown. In order to fully exploit the available data, both the scattering coefficients S_{21} and S_{12} , simultaneously measured for each resonator configuration, are fitted as S_{tr} . Indeed, although the resonator itself is a reciprocal device, the same does not hold for the whole line, because of the inevitable asymmetry of the lines between the resonator and VNAs, so that S_{21} and S_{12} are different.

The uncertainties of the uncalibrated measurements, since $u(S_{tr}) = 0$ was taken in this case, include only the contribution of the uncertainty arising from the curve fit process, as provided by the fit algorithms. This leads to the relatively low uncertainty for Q and f_0 . Very roughly, based on the available number of measured curves, an estimation of the relative uncertainty of the experimental uncalibrated data gives median values for $u_r(f_0)$ between 0.05 ppm to 0.18 ppm and for $u_r(Q)$ between 0.08 % to 0.17 %. Comparing the results with the two different fit approaches, i.e. of the complex S_{tr} and of its modulus, we obtain similar levels of the uncertainties as provided by the fit algorithms. Moreover, since these are well below the error produced by the absence of the calibration, when dealing with uncalibrated measurements the simpler fit of the modulus of S_{tr} is more than adequate and avoids unnecessary numerical complications and longer fit times.

Considering the calibrated data, the uncertainties of Q and f_0 become more than 2 times higher than for the uncalibrated case, because of the additional contribution of the known $u(S_{tr}) \neq 0$. In the following discussion we focus our attention on the calibrated data.

Comparing the results of the two fitting approaches, we

observe that, apart from providing the additional important information about the phase correction, the fit of the complex S_{tr} data is in overall characterized by a ~ 1.5 times lower u_r on the fitting parameters (Figures 3a and 4a). From Figure 3a, it can be seen that the maximum Q -factor uncertainty reduces from $u_r(Q) < 0.7\%$ for the fit of $|S_{tr}|$ to $u_r(Q) < 0.3\%$ for the fit of the complex S_{tr} . Additionally, it can be seen that that $u_r(Q)$ is almost independent on the Q -factor value. Moreover, as reasonable, $u_r(Q)$ is also independent on the VNA used for the measurement. Concerning the relative uncertainty of f_0 , the fit of $|S_{tr}|$ yields $u_r(f_0) < 1.5$ ppm which becomes lower than 0.5 ppm using the fit of the complex S_{tr} .

The comparison of the fit parameters between calibrated and uncalibrated cases can be commented using the discrepancy parameter D , reported in Figures 3b and 4b. First, since the absolute values of the discrepancy are on average larger than the uncertainties of the calibrated measurements, we can infer that they are indeed a good measure of the error due to the use of uncalibrated data.

Moreover, within the relatively large set of experimental curves, it can be observed that the discrepancy values have a balanced distribution around zero. This feature calls for a closer investigation of the characteristic of this distribution, allowing to go beyond a rough estimation of the error due to the use of uncalibrated curves as worst-case values only [10]. The latter yields as an estimate of the maximum additional contribution to the measurement relative uncertainty, arising from the use of uncalibrated data, equal to 5.4 % for Q and to 16 ppm for f_0 , but we show below that the data support a reduction of this figure.

We thus gain further information by making use of the fact, as depicted in Figures 3b and 4b, that the discrepancy is independent on the measuring device (which is not obvious, since we are dealing with uncalibrated data) and we combine together all the data for the observed discrepancies.

Analysing the statistical distribution of the D values, reported in the histograms in Figures 3c and 4c for Q and f_0 respectively, it can be seen that they yield relatively symmetric shapes centered almost in zero. In particular, for the discrepancy in f_0 its absolute mean value is 0.44 ppm for the fit of $|S_{tr}|$ and 1.9 ppm for S_{tr} fit, close to the upper value of the corresponding uncertainty of $u_r(f_0)$ in the calibrated data. For quality factor discrepancies, their absolute mean values are less than the uncertainty of $u_r(Q)$ for the calibrated data: 0.38 % for the fit of $|S_{tr}|$ and 0.16 % for the S_{tr} fit.

Interestingly, for the two fitting approaches, the standard deviations are similar: ~ 6 ppm and $\sim 2.2\%$ for the discrepancy in f_0 and Q , respectively. Since the discrepancy distributions have a dispersion, as measured by the standard deviation, much larger than their center values, given by the mean values, an estimation of the error contribution due to the use of uncalibrated data can be obtained considering the standard deviations. This allows to obtain a refined estimation of the overall uncertainty by resorting to the standard deviations of the discrepancy distributions, with respect to the above mentioned, worst-case values.

6. CONCLUSIONS

We performed an extended study on the measurement uncertainty on the quality factor and resonant frequency f_0 of microwave resonator, arising when the microwave line is not calibrated. By exploring a wide range of Q , made possible by the implementation of an ad-hoc resonator cell, we compared the

results obtained with calibrated and uncalibrated data.

We used different VNAs for data acquisition following the same procedure and different fit methods. After proper “normalizations” of the data sets, in terms of frequency span and point number, we find that while the worst case of uncertainty in calibrated curves is below 0.75 % for Q and below 1.5 ppm for f_0 , in the uncalibrated measurements an additional contribution arises.

By estimating this contribution from the discrepancy between the fit results of calibrated and uncalibrated data, we obtain an experimental quantification of the additional contribution equal to 5.4 % for Q and 16 ppm for f_0 as a maximum error. By combining all the data for the discrepancy,

we can reduce this figure to 2.2 % and 6 ppm, respectively, that now should be intended as standard uncertainties. These results provide a guide for the evaluation of the uncertainty contribution to be taken into account when calibration of microwave lines similar to the one studied are not feasible.

REFERENCES

[1] S. Chen et al., A Dielectric Constant Measurement System for Liquid Based on SIW Resonator, IEEE Access, 6 (2018), pp 41163-41172.
 [2] Schultz, J. W., A New Dielectric Analyzer for Rapid Measurement of Microwave Substrates up to 6 GHz, Proc. of AMTA 2018, Williamsburg, 4-9 Nov 2018, pp. 1-6.

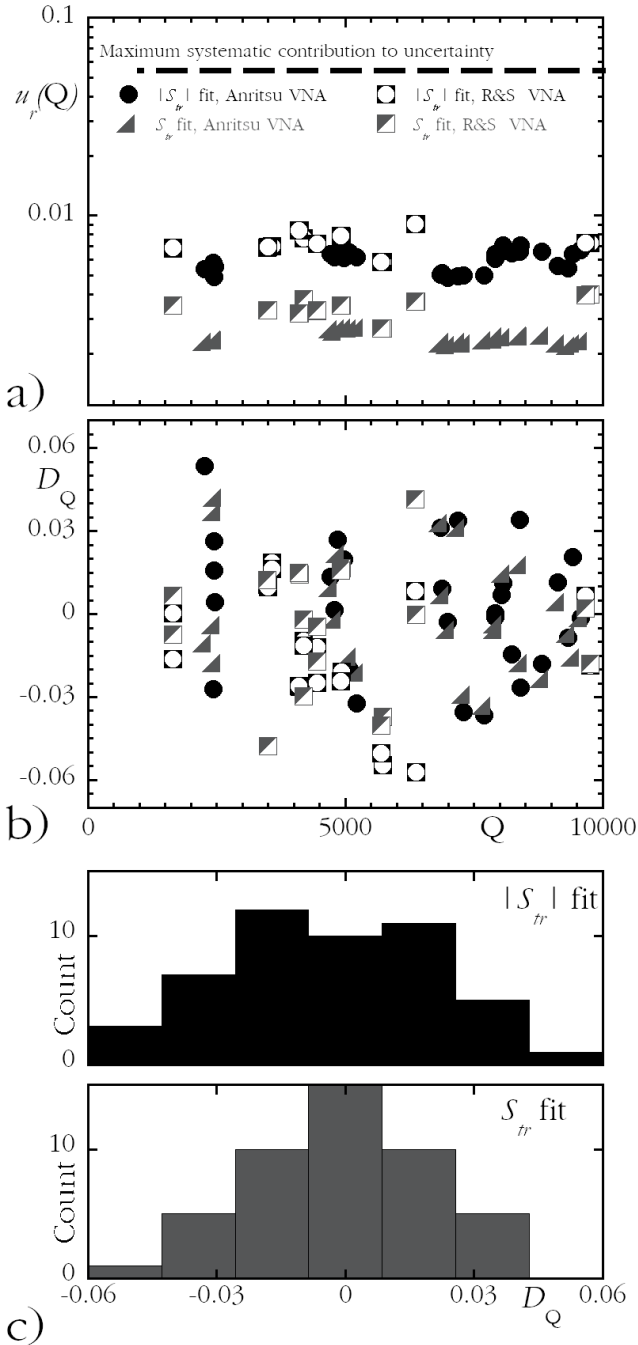


Figure 3. Panel a): relative uncertainty on calibrated Q -factor vs Q . Panel b): discrepancy D_Q vs Q . Panel c): distribution of the discrepancy D_Q .

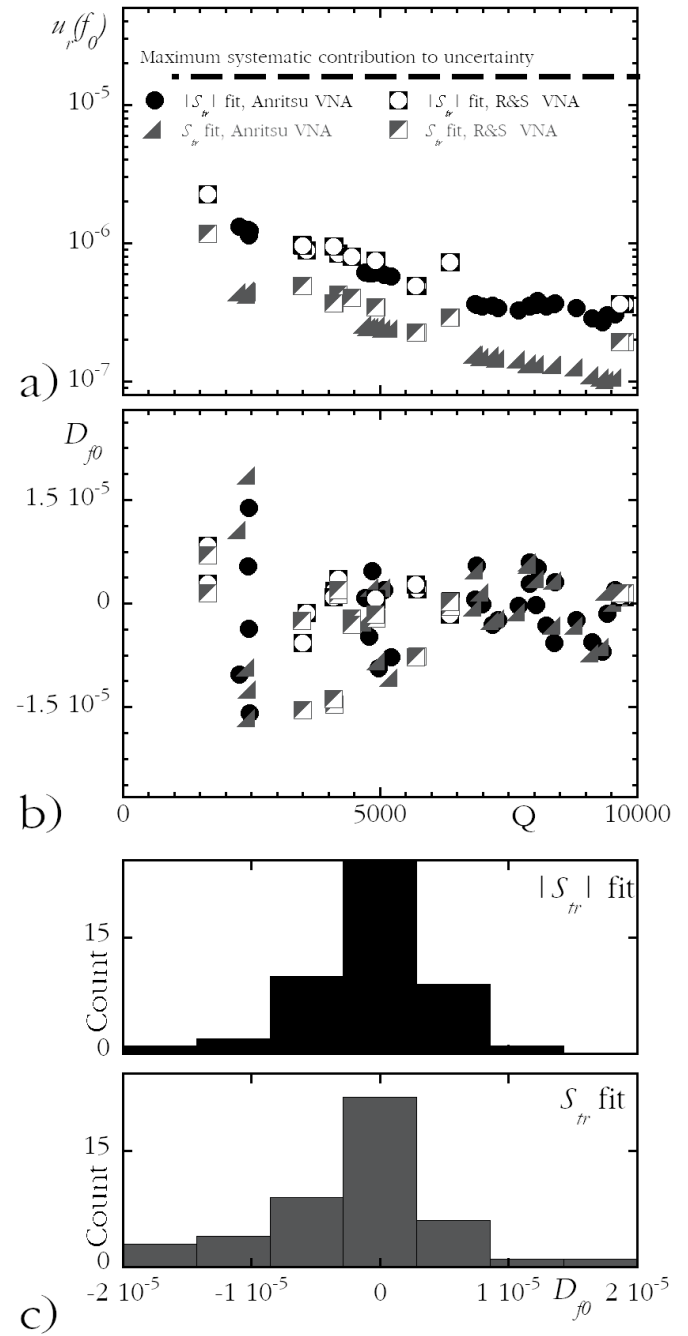


Figure 4. Panel a): relative uncertainty on calibrated f_0 vs Q . Panel b): discrepancy D_{f_0} vs Q . Panel c): distribution of the discrepancy D_{f_0} .

- [3] IEC 61788-7:2006, Superconductivity - Part 7: Electronic characteristic measurements - Surface resistance of superconductors at microwave frequencies.
- [4] A. Frolova et al., Critical current and vortex pinning properties in $\text{YBa}_2\text{Cu}_3\text{O}_{7-x}$ films with $\text{Ba}_2\text{YTaO}_6+\text{Ba}_2\text{YNbO}_6$ and BaZrO_3 nanoinclusions by DC transport and microwave measurements, *IEEE Trans. Appl. Supercond.*, 28 (2018), Art. ID 7500805.
- [5] K. Will, T. Meyer and A. Omar., Low-cost high-resolution handheld VNA using RF interferometry, 2008 IEEE MTT-S International Microwave Symposium Digest, Atlanta, GA, 15-20 June 2008, pp. 375-378.
- [6] T. Sokoll and A. F. Jacob, Self-calibration circuits and routines for low-cost measuring systems, *Microw. Opt. Technol. Lett.*, 50 (2008), pp. 287-293.
- [7] A. Alimenti et al., Surface Impedance Measurements on Nb_3Sn in High Magnetic Fields, *IEEE Trans. Appl. Supercond.*, 29 (2019), Art. ID 3500104.
- [8] A. Alimenti et al., Challenging microwave resonant measurement techniques for conducting material characterization. *Measurement Science and Technology*, 30 (2019), Art. ID 065601.
- [9] M. Scheffler and M. Dressel, Broadband microwave spectroscopy in Corbino geometry for temperatures down to 1.7 K, *Rev. Sci. Instrum.*, 76 (2005), Art. ID 074702; M. Scheffler et al., Broadband Corbino spectroscopy and stripline resonators to study the microwave properties of superconductors, *Acta IMEKO*, 4 (2015), pp. 47-52.
- [10] K. Torokhtii et al., Q-factor of microwave resonators: calibrated vs. uncalibrated measurements, *J. Phys. Conf. Ser.*, 1065 (2005), Art. ID 052027.
- [11] K. Torokhtii, A. Alimenti, N. Pompeo and E. Silva, Uncertainty in uncalibrated microwave resonant measurements, *Proc. of the XXIII IMEKO TC4 International Symposium Electrical & Electronic Measurements Promote Industry Xi'an, China*, 17 – 20 September 2019, pp. 98-102. ISBN: 978-606-13-5238-8.
- [12] Embedding/De-embedding, Anritsu Application Note, 2002.
- [13] N. Pompeo, K. Torokhtii, E. Silva, Dielectric resonators for the measurements of the surface impedance of superconducting films, *Meas. Sci. Rev.*, 14 (2014), pp. 164-170.
- [14] N. Pompeo et al., Fitting strategy of resonance curves from microwave resonators with non-idealities, *Proc. of I2MTC 2017 - 2017 IEEE International Instrumentation and Measurement Technology Conference*, *J. Phys. Conf. Ser.*, Torino, Italy, 22 - 25 May 2017, pp. 1-6.
- [15] J. W. Yoon, and R. Magnusson, Fano resonance formula for lossy two-port systems, *Opt. Express*, 21 (2013), pp. 17751-17759.
- [16] P. J. Petersan and S. M. Anlage, Measurement of resonant frequency and quality factor of microwave resonators: Comparison of methods, *J. Appl. Phys.*, 84 (1998), pp. 3392-3402.
- [17] K. Leong and J. Mazierska, Precise measurements of the Q factor of dielectric resonators in the transmission mode-accounting for noise, crosstalk, delay of uncalibrated lines, coupling loss, and coupling reactance, *IEEE Trans. Microw. Theory Tech.*, 50 (2002), pp. 2115-2127.
- [18] M. Žic, An alternative approach to solve complex nonlinear least-squares problems, *J. Electroanal. Chem.*, 760 (2016), pp. 85-96.
- [19] J. J. More, B. S. Garbow and K. E. Hillstrom, User Guide for MINPACK-1, Argonne National Laboratory, Argonne, Ill., 1980.
- [20] www.anritsu.com
- [21] M. Wollensack, J. Hoffmann, J. Ruefenacht, and M. Zeier, VNA Tools II: S-parameter uncertainty calculation, *Proceedings of 79th ARFTG Microwave Measurement Conference*, Montreal, Canada, 22 June 2012, pp. 1-5.
- [22] E. Jones, E. Oliphant, P. Peterson et al., *SciPy: Open Source Scientific Tools for Python*, 2001, https://docs.scipy.org/doc/scipy/reference/generated/scipy.optimize.curve_fit.html.